Submitted, accepted and published by

Energy & Fuels 2006, 20, 26-33

Effect of pressure on the behavior of Copper-, Iron-and Nickel-based Oxygen Carriers for Chemical-Looping Combustion

Francisco García-Labiano, Juan Adánez, Luis F. de Diego, Pilar Gayán, and Alberto Abad*

Department of Energy and Environment, Instituto de Carboquímica (CSIC), Miguel Luesma Castán 4, 50018 Zaragoza, Spain

E-mail: glabiano@icb.csic.es

* Corresponding author. Tel.: +34-976733977. Fax: +34-976733318. E-mail: glabiano@icb.csic.es

The combustion process integrated by coal gasification and chemical-looping combustion (CLC) could be used in power plants with low energy penalty for CO_2 capture. This work analyses the main characteristics related with the CLC process necessary to use the syngas obtained in an integrated gasification combined cycle (IGCC) power plant. The kinetics of reduction with H_2 and CO, and oxidation with O_2 of three high reactivity oxygen carriers used in the CLC system have been determined in a thermogravimetric analyzer at atmospheric pressure. The iron- and nickel-based oxygen carriers were prepared by freeze-granulation, and the copper-based oxygen carrier was prepared by impregnation. The changing grain size model (CGSM) was used for the kinetic determination, assuming spherical grains for the freeze-granulated particles based on iron and nickel, and plate-like geometry for the reacting surface of the copper-based impregnated particles. The dependence of the reaction rates

with temperature was low, with the activation energies values varying from 14 to 33 kJ mol^{-1} for the reduction, and from 7 to 15 kJ mol^{-1} for the oxidation. The reaction order depended on the reacting gas and oxygen carrier, with values ranging from 0.25 to 1.

However, an increase in the operating pressure for the IGCC+CLC system increases the thermal efficiency of the process and the CO_2 is recovered as a high pressure gas, decreasing the energy demand for further compression. The effect of pressure on the behavior of the oxygen carriers has been analyzed in a pressurized thermogravimetric analyzer at 1073 K and pressures up to 30 atm. It has been found that an increase in total pressure has a negative effect on the reaction rates of all the oxygen carriers. Moreover, the use of the CGSM with the kinetic parameters obtained at atmospheric pressure predicted higher reaction rates than the experimentally obtained at higher pressures and therefore the kinetic parameters necessary to design pressurized CLC plants must be determined at the operating pressure.

KEYWORDS: Kinetics, Chemical-Looping Combustion, Pressure

Introduction

Increasing concentrations of CO_2 and other greenhouse gases in the atmosphere are enhancing the natural greenhouse effect, leading to changes in the climate. The nature, extent and timing of these changes are uncertain but one of the main changes is expected to be a rise in the global average temperature of earth. It is generally accepted therefore that a reduction in emissions of greenhouse gases is necessary as soon as possible. The increase of efficiency of energy conversion as well as increasing the use of renewable sources (biofuel, wind power, etc.) will not be enough to cover the increasing energy demand, and fossil fuels will be the dominant energy source worldwide in the short and medium term.[1] Among them, coal has considerable larger resources than oil and natural gas. A strategy to decrease emissions of greenhouse gases in combustion processes is CO_2 capture and sequestration; however, conventional gas separation techniques in diluted streams have been estimated to be rather costly and decrease the net power efficiency of the plant.[2]

In this sense, a process integrated by coal gasification and chemical-looping combustion (CLC) could be used in power plants with low energy penalty for CO_2 capture.[3-5] Simulations made by Jin and Ishida[6] and Wolf et al.[7] showed that this process have the potential to achieve an efficiency of about five percentage points higher than a similar combined cycle that uses conventional CO_2 capture technology.[8] It must be also considered that different economic assessments performed in the framework of the GRACE project for a 200 MWth chemical-looping combustion boiler for use at BP´s Grangemouth refinery, and by the CO_2 Capture Project (CCP) indicated CLC among the best options for reducing the cost of CO_2 capture using fuel gas.[9-10]

CLC is a two-step gas combustion process that produces a pure CO_2 stream, ready for compression and sequestration. A solid oxygen carrier circulates between two fluidized bed reactors and transports oxygen from the combustion air to the fuel. Since the fuel is not mixed with air, the subsequent CO_2 separation process is not necessary. As gaseous fuel can be used natural gas or synthesis gas from coal gasification.

The fuel, e.g. syngas, is introduced to the fuel reactor, where it is oxidized by the oxygen carrier, i.e. the metal oxide, MeO. The exit gas stream from the fuel reactor contains CO_2 and H_2O, and almost pure CO_2 is obtained after H_2O condensation. The particles of the oxygen carrier are transferred to the air reactor where they are regenerated by taking up oxygen from the air. The exit gas stream from the air reactor contains N_2 and some unused O_2. The total amount of heat evolved from reactions in the two reactors is the same as for normal combustion, where the oxygen is in direct contact with fuel.

The key issue in the system performance is the oxygen carrier material. Iron, nickel, and copper have been selected as the most promising metals to be used in a CLC process. Oxides of these metals supported on several inerts have been found to react with sufficiently high rates during successive reduction-oxidation cycles to be used for CLC.[11-14] Besides high reactivity, the oxygen carriers must fulfill other characteristics as high resistance to attrition and no presence of agglomeration.

Coal gasification is a well established technology for the production of synthesis gas. The adoption of pressurized operation for gasifiers, as in the integrated gasification combined cycle (IGCC) systems for

utility power generation, allows the increase of the thermal efficiencies.[1] The use of a pressurized CLC system would have several advantages. First, the efficiency of the cycle in the CLC power plant will be increased;[7] second, the recovering of the CO_2 as a high-pressure gas requires only a very small amount of additional power for further compressing the CO_2 to pipeline (35 atm) or sequestration pressure (100 atm).[4]

So far, very limited work on the behavior of the oxygen carriers under pressurized conditions has been done. Copeland et al.[4] made multiple cycle testing of their materials in a small-scale fluidized bed reactor up to 100 psig, and at higher scale in a pilot-scale fluidized bed reactor. Jin and Ishida[5,15] made experiments to know the behavior of several oxygen carriers in a thermogravimetrical reactor and in a fixed-bed reactor at pressures up to 10 bars. Ryu et al.[16] presented a preliminary design of a 50 kWth unit based on a pressurized fluidized bed technology. Recently, Wolf et al.[17] have analyzed the feasibility of CLC in two interconnected pressurized fluidized bed reactors using natural gas as fuel, and pressures from 9 to 13 bars. They mentioned the reaction kinetics as one of the most important technical constrains of the oxygen carriers from the point of view of the system's performance.

The objective of this work was to analyze the effect of pressure on the reaction rate of three oxygen carriers, based on copper, iron, and nickel; and determine the kinetic parameters in their reactions with H_2, CO, and O_2.

Experimental Section

Material. Three oxygen carriers using Al_2O_3 as support were used in this work: particles of copper (II) oxide prepared by impregnation (Aldrich Chemical Company), and iron- and nickel-based particles prepared by freeze-granulation[18] at Chalmers University of Technology. The samples were designated as Cu10Al-I, Fe45Al-FG, and Ni40Al-FG. In all cases, part of the metal oxide used in the preparation reacts with the support to give aluminates and it was not active for reaction. The samples were characterized by Hg porosimetry, and N_2 physisorption to determine the internal structure of the particles, and by scanning electron microscopy using energy-dispersive X-ray (SEM-EDX) to determine

the dispersion of the metal oxide inside the particles. Table 1 shows the main physical characteristics of the materials. The oxygen transport capacity, R_0, of the oxygen carriers depends both on the active metal oxide content, and on the type of metal oxide considered. In this sense, the value of R_0 for pure metal oxides is higher for the NiO/Ni (0.21) and CuO/Cu (0.20), than for the Fe_2O_3/Fe_3O_4 (0.03) or $Fe_2O_3/Fe_{0.947}O$ (0.08) transformations.

Table 1. Properties of the oxygen carriers.

	Cu10Al-I	Fe45Al-FG	Ni40Al-FG
Active MeO content (wt %)	10	45	40
Particle size (mm)	0.17	0.15	0.2
Porosity	0.57	0.30	0.36
Specific surface area BET ($m^2\ g^{-1}$)	41.3	2.5	0.8
Apparent density (kg m^{-3})	1800	3257	3446
Oxygen transport capacity, R_0	0.02	0.013	0.084

Experimental set-up. The kinetic of the reduction and oxidation reactions of the oxygen carriers has been determined in an atmospheric CI thermobalance. More details about the experimental system and operating procedure can be found elsewhere.[19] The experiments at higher pressure were carried out in a pressurized thermogravimetric analyzer (PTGA), Cahn TG-2151 type (Figure 1). The thermobalance consists of a quartz tube (31 mm i.d.) placed in an oven that can be operated at pressurized conditions. The sample holder, to reduce mass transfer resistance around the sorbent sample was a wire mesh platinum basket (11 mm diameter and 4 mm height). Temperature, pressure, and sample weight were continuously measured and recorded on a computer. The reacting gas mixture (83 $cm^3\ s^{-1}$ STP) containing H_2/N_2, or $CO/CO_2/N_2$, or O_2/N_2 were controlled by electronic mass flow controllers. Due to condensation problems in the lower part of the PTGA it was not possible to feed water into the system. On the other hand, CO_2 was introduced together with CO to avoid carbon formation by the Boudouard reaction.

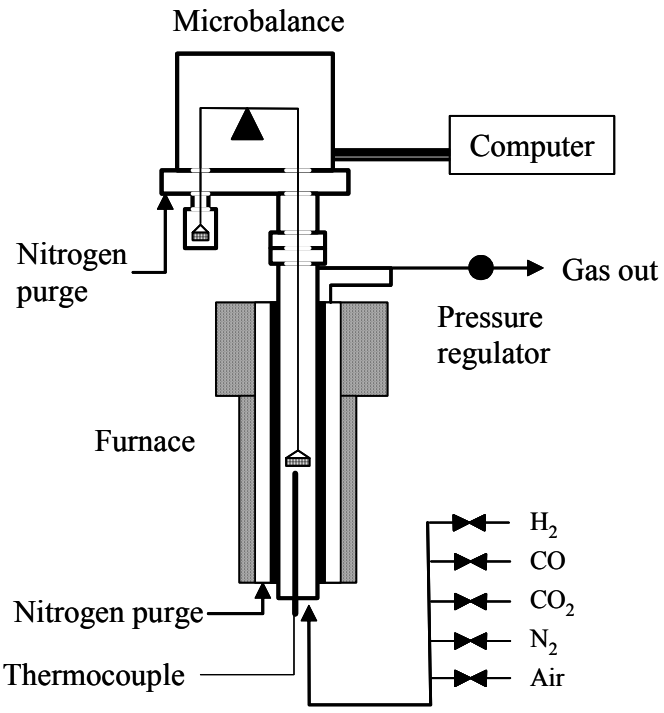

Figure 1. Pressurized thermogravimetric analyzer system, PTGA.

Procedure. To minimize the mass transfer resistance between particles, the sample (30-70 mg) was loaded between layers of quartz wool in the platinum basket. The oxygen carriers were heated in air up to the desired temperature and then the system was pressurized. The experiment started by exposing the oxygen carrier to alternating reducing and oxidizing conditions. To avoid the mixing of combustible gas and air, nitrogen was introduced for two minutes after each reacting period.

The experiments were carried out at 1073 K and different total pressures up to 30 atm. Five cycles of reduction and oxidation were normally carried out for each experimental condition. The sample normally stabilized after the first cycle, for which the reduction reaction was usually slower than the obtained in the following cycles.

Gas dispersion in the PTGA. A common problem in the use of PTGA is that the inlet gas flow is limited by the disturbances produced in the weight signal when high pressures are used. For the maximum gas flow used in the PTGA system at high pressures, the assumption of gas plug flow is not correct and the gas concentration around the particles is not constant during the initial stages of reaction. To determine the gas dispersion in the PTGA system, a gas analyzer was located at the outlet of the

system, after the pressure control valve. A gas tracer step input allowed us to know both the time spent by the gas to reach the analyzer and the F curve of the whole system at different total pressures.[20] However, the sample was located in an intermediate place between the gas feeding and the gas outlet from the system, and the gas dispersion in that location was calculated with the equations for non-ideal flows in practical reactors.[20-21] Figure 2 shows the gas concentration around the sample particles as a function of time for different pressures, working at the maximum stable flowrate (83 cm^3 s^{-1} STP). The times necessary to reach the desired concentration varied from ≈1 s at atmospheric pressure up to ≈40 s at 30 atm. The relative importance of the gas dispersion will depend on the reaction rate of the oxygen carrier with the gas, and it will be analyzed below for each case.

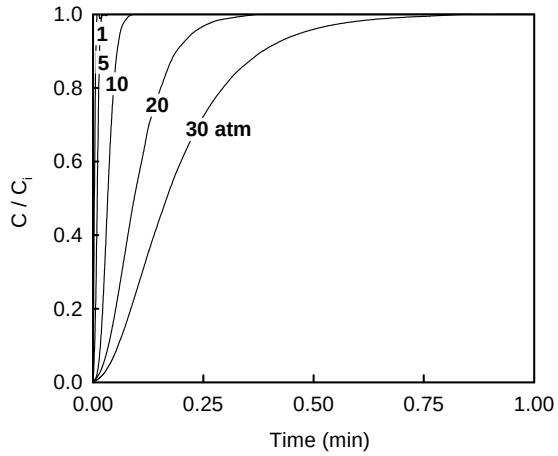

Figure 2. Real gas concentration around the particles at different pressures.

Data evaluation. The reduction and oxidation reactions of an oxygen carrier per mol of fuel gas are given by the following equations

$$b\ MeO + CO \longrightarrow a\ Me + CO_2 \quad (1)$$

$$b\ MeO + H_2 \longrightarrow a\ Me + H_2O \quad (2)$$

$$b\ Me + O_2 \longrightarrow c\ MeO \quad (3)$$

where Me represents a metal or a reduced form of MeO. Table 2 shows the values of the b parameter, used later in the kinetic model, for the different oxygen carriers and reactions. The conversion level of the oxygen carrier was calculated as:

For reduction, $X_s = \frac{m_{ox} - m}{m_{ox} R_0}$ (4)

For oxidation, $X_s = 1 - \frac{m_{ox} - m}{m_{ox} R_0}$ (5)

The oxygen transport capacity of the oxygen carriers, R0, used in this work are given in Table 1.

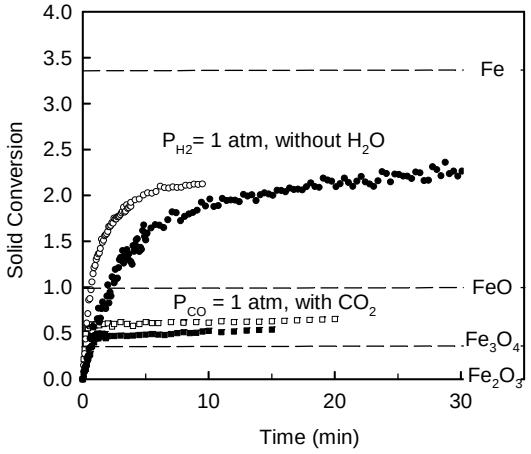

Figure 3. Effect of the reacting gas on the final product reached on Fe_2O_3 reduction. Total pressure: ○,□ 5 atm; ●,■, 20 atm. FeO was considered as the reference material for solid conversion calculations.

Iron compounds needs special attention due to their different oxidation states (Fe_2O_3-Fe_3O_4-FeO-Fe). Depending on gas composition, the reduction of Fe_2O_3 can finish in one of the above products, and consequently, the value of R_0 will be very different depending on the reaction considered. Figure 3 shows the reduction curves obtained for the Fe45Al-FG oxygen carrier with different reacting gases and operating conditions. In a real CLC system, H_2O is produced during the Fe_2O_3 reduction with H_2. The thermodynamic equilibrium shows that for typical values of H_2O and H_2 concentrations, the final product would be normally Fe_3O_4 or FeO. However, the impossibility to feed H_2O in our PTGA system made that the final product was Fe when using H_2 as fuel gas. On the other hand, FeO was reached when CO-CO_2 was used for the reduction. However, only the transformation from hematite to magnetite (Fe_2O_3 - Fe_3O_4) may be applicable for industrial CLC systems. Further reduction to FeO would produce a high decrease in the CO_2 purity obtained in the fuel reactor because of the increase in the equilibrium concentrations of CO and H_2.[4, 22] Because in the TGA system it was not possible to stop the reaction in

the Fe_3O_4 product, the first part of the experimental curves was used to determine the kinetic of the reaction from Fe_2O_3 to Fe_3O_4. On the other hand, the oxidation curves depended on the final products obtained during the reduction step. In this work, only the oxidations corresponding to the transformation FeO-Fe_2O_3 were considered.

Kinetic model

There are several resistances that can affect the reaction rate of the oxygen carrier with the fuel gas or with the air. Previous calculations showed that the mass transfer resistances in the gas film and in the product layer of the particle were not important in the experimental conditions used in this work. Moreover, several experiments showed that the particle size in the range 0.09-0.250 mm did not affect the reaction rates.

The changing grain size model (CGSM)[23] was used to predict the evolution with time of the reduction and oxidation reactions. Two different geometries were considered taking into account the structural differences of the oxygen carriers. SEM-EDX analysis of the samples showed a granular structure in the Fe- and Ni-based oxygen carriers prepared by freeze-granulation.[24] On the other hand, the analysis of the Cu-based oxygen carriers showed that the CuO was well dispersed in the porous surface of the alumina matrix, and a uniform layer of metal oxide can be considered.[19] In this case, the shrinking core model for plate-like geometry in the porous surface of the particle was used. The equations that describe the CGSM are the following:

Chemical reaction

Spherical grains

$$\frac{t}{\tau} = 1-(1-X)^{1/3} \qquad \tau = \frac{\rho_m\, r}{b\, k\, (C^n - C_{eq}^n)} \tag{6}$$

Plate-like geometry

$$\frac{t}{\tau} = X \qquad \tau = \frac{\rho_m\, L}{b\ \ k\, C^n} \tag{7}$$

where the preexponential factor follows an Arrhenius type dependence with temperature

$$k = k_0 \, e^{-E/RT} \quad (8)$$

The grain radius of the freeze-granulated particles was calculated from porosity and specific surface area measurements (see Table 1). The thickness of the layer, L_i, in the Cu-based oxygen carrier prepared by impregnation was determined considering the active surface area obtained by H_2 chemisorption. Equation 6 considers the thermodynamic equilibrium that occurs in the Ni-based oxygen carriers working with H_2 or CO. For the other metal oxides the value of C_{eq} is zero.

Results and Discussion

The kinetics of the reduction and oxidation reactions of the three oxygen carriers were determined in a thermobalance (CI Electronics Ltd.) at atmospheric pressure.[19, 25] The gas dispersion in the system was negligible at the operating conditions, and gas plug flow was considered. Temperatures from 723 K to 1223 were used. The composition of the gas during metal oxide reduction was varied to cover the majority of the gas concentrations present in the fluidized-bed fuel reactor of a CLC system (fuel, 5-70 vol %; H_2O, 0-48 vol %; CO_2, 0-40 vol %). For the oxidation reaction, oxygen concentrations from 5 to 21 vol % were used.

The use of the CGSM together with the experimental data allowed us to obtain the kinetic parameters corresponding to the different reactions for the several oxygen carriers (see Table 2). The reactions were fitted assuming kinetic control, with the only exception of the NiO reduction with H_2, where an additional diffusion resistance was used. However, the effect of this resistance on the reaction rate could be considered negligible in practical conditions at temperatures above 1073 K. The effect of temperature was low in all cases, with the activation energies values varying from 14 to 33 kJ mol^{-1} for the reduction, and from 7 to 15 kJ mol^{-1} for the oxidation. The reaction order depended on the reaction and oxygen carrier considered, and values from 0.25 to 1 were found. No effect of the gas products (H_2O or CO_2) on the reduction reaction rates was detected.

Table 2. Kinetic parameters for the investigated oxygen carriers.

	Cu10Al-I			Fe45Al-FG			Ni40Al-FG		
	H_2	CO	O_2	H_2	CO	O_2	H_2	CO	O_2
Physical parameters									
ρ_m (mol/m^3)	80402	80402	140251	32811	32811	22472	89290	89290	151520
r or L (m)	$4.0\ 10^{-10}$	$4.0\ 10^{-10}$	$2.3\ 10^{-10}$	$2.6\ 10^{-7}$	$2.6\ 10^{-7}$	$2.6\ 10^{-7}$	$6.9\ 10^{-7}$	$6.9\ 10^{-7}$	$5.8\ 10^{-7}$
b	1	1	2	3	3	4	1	1	2
Kinetic parameters *									
k_0 (mol^{1-n} m^{3n-2} s^{-1})	$1.0\ 10^{-4}$	$5.9\ 10^{-6}$	$4.7\ 10^{-6}$	$2.3\ 10^{-3}$	$6.2\ 10^{-4}$	$3.1\ 10^{-3}$	$9.3\ 10^{-3}$	$5.2\ 10^{-3}$	$1.8\ 10^{-3}$
E (kJ/mol)	33	14	15	24	20	14	26	25	7
n	0.6	0.8	1.0	0.8	1.0	1.0	0.5	0.8	0.2
Effect of pressure									
d	0.53	0.83	0.68	1.03	0.89	0.84	0.47	0.93	0.46

* Obtained at atmospheric pressure.

To analyze the effect of total pressure on the behavior of the oxygen carriers, two kinds of experiments were carried out in the PTGA. First, experiments with a constant molar fraction (10 vol %) of reducing gas, CO or H_2, and different total pressures up to 30 atm were performed at 1073 K. Figure 4 shows, as an example, the results obtained during the reduction with CO of the Ni-based oxygen carrier. Since an increase in the operating pressure represents also an increase in the reacting gas partial pressure, an increase in the reaction rate of the oxygen carriers would be expected. However, a small decrease in the reaction rate with increasing pressure was detected for all the oxygen carriers and reactions analyzed in this work. It must be considered, however, that the experimental data are the result of several effects acting together: total pressure, partial pressure, and gas dispersion. The effect of gas dispersion will be analyzed below with more detail.

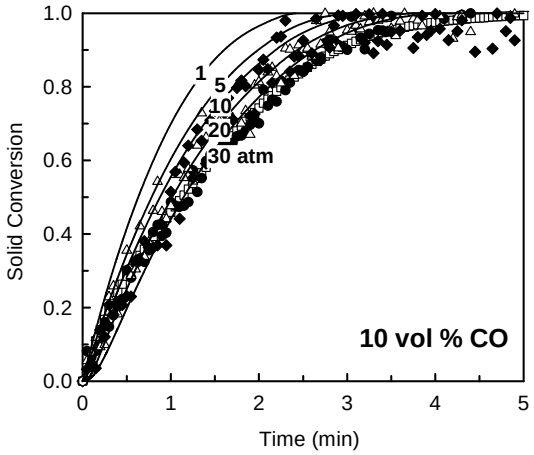

Figure 4. Effect of total pressure on the reduction of Ni-based oxygen carrier with a constant molar fraction of CO (10 vol %). CO_2=10 vol %. 1073 K. Experimental data: □ 1 atm, ● 5 atm, △ 10 atm, ◆ 20 atm, ○ 30 atm. Continuous lines = model predictions considering the effect of pressure and gas dispersion.

To deeply analyze the effect of operating pressure, other experiments were performed with a constant gas partial pressure of 1 atm and different total pressures. The oxidation data corresponding to 1 atmosphere of total pressure were not obtained because we used air as reacting gas. Figure 5 shows the results obtained at 1073 K for the different oxygen carriers and reaction gases. A sharp decrease of the reaction rate with increasing total pressure was observed in all cases. This negative effect of pressure has been also observed by other authors in several gas-solid reactions, as will be showed below.[26-31] The results were again affected by the gas dispersion in the system although their effect was low, as will be showed below.

The reaction rate of the oxygen carriers with H_2 was always higher than the obtained with CO. The oxidation reaction rates were high, similar to the reductions with H_2, and did not depend on the gas used for the reduction.

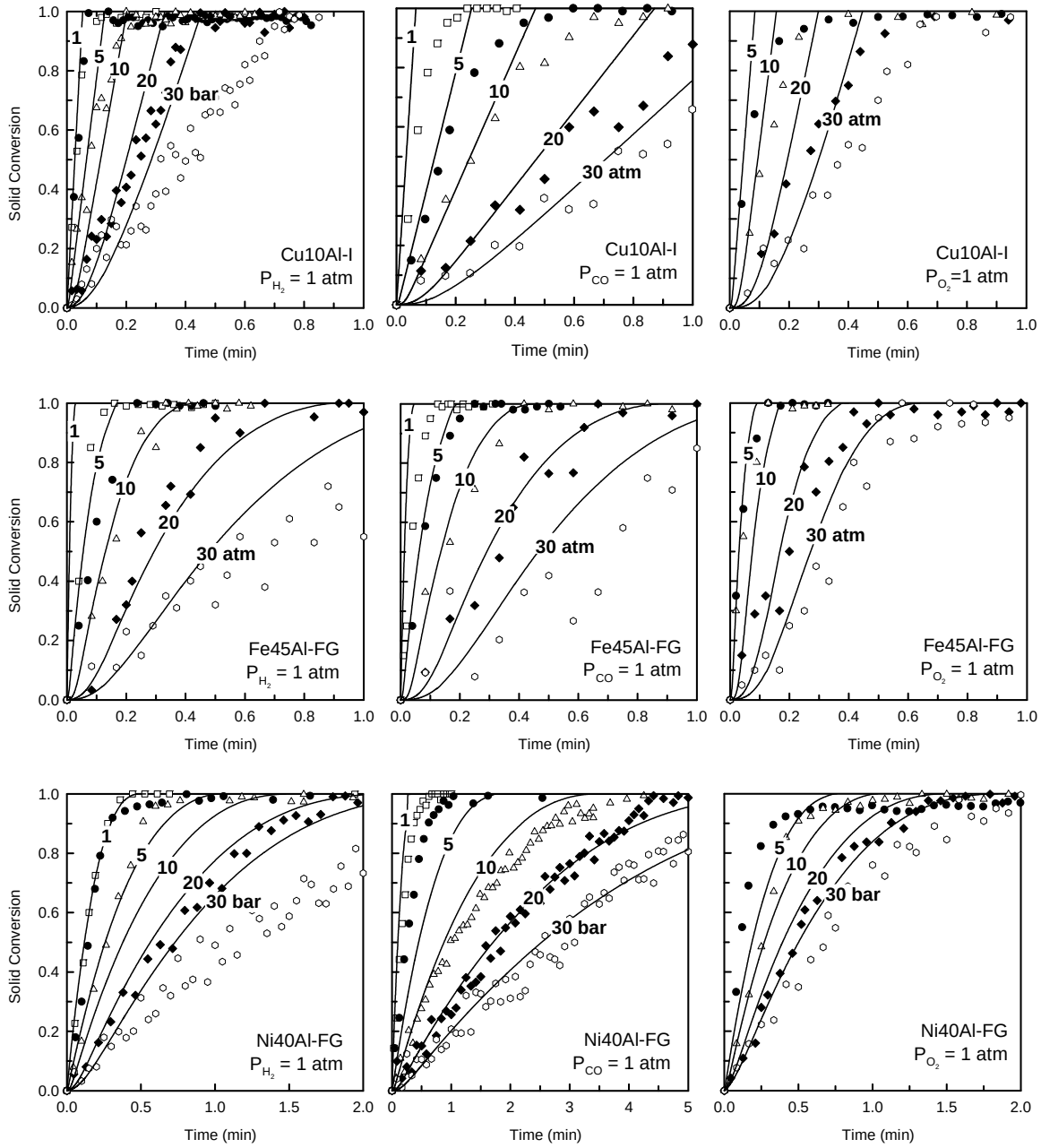

Figure 5. Effect of total pressure on the reduction and oxidation reactions of different Cu-, Fe- and Ni-based oxygen carriers with a constant partial pressure of gas (P_p=1 atm). 1073 K. Experimental data: □ 1 atm, ● 5 atm, △ 10 atm, ◆ 20 atm, ○ 30 atm. Continuous lines = model predictions considering the effect of pressure and gas dispersion. For the iron compounds, the solid conversion corresponds to the transformation Fe_2O_3-Fe_3O_4.

A comparison between materials showed that the Cu-based oxygen carrier exhibited the highest reaction rate, followed by the Ni- and the Fe-based oxygen carriers. Besides the type of metal oxide

considered, this phenomenon seems to be related with the metal oxide dispersion and internal structure (solid porosity and specific surface area) of the oxygen carrier. These characteristics are affected by the preparation method, inert type, sintering temperature and metal oxide content in the oxygen carrier.[13] It must be considered that the Fe- and Ni-based particles were prepared by freeze-granulation while Cu-based particles were prepared by impregnation.

Effect of pressure on kinetic parameters. Because of the gas dispersion existing in the PTGA system at high pressures, the reactivity data were obtained with a non-constant concentration, and eqs. (6) - (7) could not be directly used to determine the kinetic parameters. However, it was possible to know the instantaneous reaction rates, dX/dt, obtained with the real gas concentrations around the sample particles showed in Figure 2. The theoretical conversions versus time curves were obtained by integration of the instantaneous reaction rate values.

The use of CGSM and the kinetic parameters obtained at atmospheric pressure together with the real gas concentrations around the particles, which were obtained considering the gas dispersion in the system, were unable to predict the experimental results obtained at pressure. Figure 6 shows an example of the model predictions and experimental data at different total pressures when the partial pressure of CO was maintained constant for the reduction of the Ni40Al-FG oxygen carrier. In all cases, the use of the kinetic parameters obtained at atmospheric pressure predicted reaction rates much higher than the experimentally obtained. This behavior was obtained for all reactions and oxygen carriers. The differences in the model predictions observed in Figure 6 for the curves at constant partial pressure are due to the gas dispersion existing at the different operating pressures.

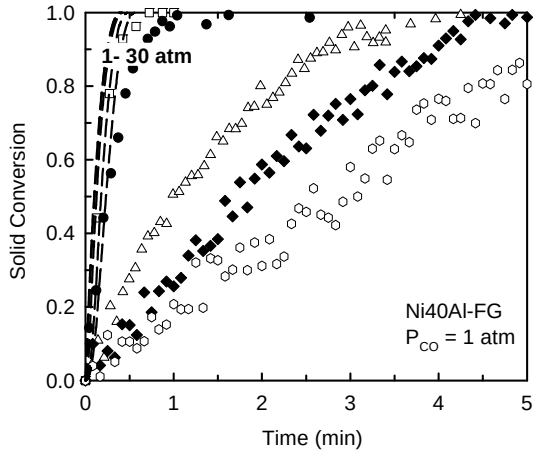

Figure 6. Comparison between experimental data (symbols) and CGSM predictions using the kinetic parameters obtained at atmospheric pressure and considering the gas dispersion in the system (Discontinuous lines). Experimental data: □ 1 atm, ● 5 atm, △ 10 atm, ◆ 20 atm, ○ 30 atm.

Several authors have observed the negative effect of the increasing total pressure on gas-solid reactions and have proposed different explanations. Matsukata et al.[26] developed an empirical model in which the apparent kinetic rate constant varied with total pressure and conversion. Agnihotri et al.[27] proposed that the increase of moles of gas produced during the sulfidation of non-calcined Ca-based sorbents was the responsible of the effect of pressure. This reason is not valid in this case because the number of moles of gas remains constant in the CLC reactions with synthesis gas. Qiu and Lindqvist[28] observed that both the kinetic rate constant and the effective diffusivity of SO_2 through the product layer obtained in their study about the sulfation reaction decreased as the total pressure increased. Qiu et al.[29] explained the effect of total pressure on the oxidation reaction of CaS to $CaSO_4$ by the inhibition of the gas diffusion in the porous system of the particles. García-Labiano et al.[30] used a dependence with total pressure in the effective diffusivity in the pores and in the product layer to predict their experimental results about sulfidation of sorbents.

However, the use of the CGSM to the CLC reactions, including the internal gas diffusion in the pores[32] and considering the inhibition of the gas diffusion in the porous system of the particles,[33] neither was valid to predict the experimental results obtained in this work at pressurized conditions. On the other hand, Chauk et al.[31] observed that the sulfidation conversion was adversely affected by increasing

pressure due to CaO sorbent morphological alterations, such as reduction in surface area and pore volume. This aspect was not corroborated in this work because the amount of sample used in the PTGA experiments was not enough to determine the physical characteristics of the materials after reaction at the different pressures. In our case, this fact would drive to the use of a different grain size at each CLC operating pressure.

Although it would be recommendable to determine the kinetic parameters at the same operating pressure to be used in the CLC plant, to know the magnitude of the effect of total pressure on the decrease of the reaction rates, an empirical fit was done. The value of the preexponential factor at each pressure, $k_{0,p}$, that best fit the experimental data considering the gas dispersion was obtained for each oxygen carrier and reaction. Figure 7 shows the $k_{0,p}/k_0$ values obtained for all reactions as a function of total pressure. In the majority of the cases, a sharp decrease in the value of $k_{0,p}$ was observed when the pressure changed from 1 to 5 atm, with a smoother decrease for increasing pressures. For some reactions the decrease was softer, although in any case the values of $k_{0,p}$ at 30 atm were between 5 and 95 times lower than at atmospheric pressure. Finally, an apparent preexponential factor was determined as a function of total pressure and the preexponential factor obtained at atmospheric pressure

$$k_{0,p} = \frac{k_0}{P^d} \qquad (9)$$

Table 2 shows the values of the parameter "d" obtained for the different oxygen carriers and reacting gas. In this way it was possible to predict the experimental results, showed as continuous lines in Figures 4 and 5, within the range of total pressures used.

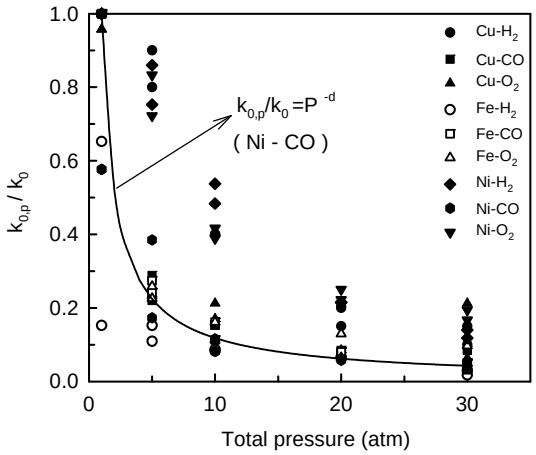

Figure 7. Effect of total pressure on the decrease of the preexponential factor for the different oxygen carriers and reactions. Continuous line = Example of the fit of the apparent preexponential factor corresponding to the reaction of the Ni40Al-FG oxygen carrier with CO according to equation (9).

Effect of gas dispersion. As showed in Figure 2, the gas dispersion in the experimental system was determined at the different operating pressures. The relative importance of this effect depended on the reaction rate of the oxygen carrier with the gas. Figure 8 shows an example of the dX/dt values for two different cases, when the gas dispersion was considered or when the gas dispersion was neglected. For the slowest reaction, i.e. Ni45Al-FG reduction with CO, the gas dispersion hardly affected the reaction rates at the beginning of the reaction. However, for the quickest reactions, i.e. Cu10Al-I reduction with H_2, the gas dispersion in the system affected the reaction rate values during a long part of the reaction time. In the extreme case, at 30 atm, the reaction had finished before reach the desired gas concentration in the sample basket. Therefore, the gas dispersion of the system affects the reaction rate and must be considered, as it was done in this work to fit the experimental data.

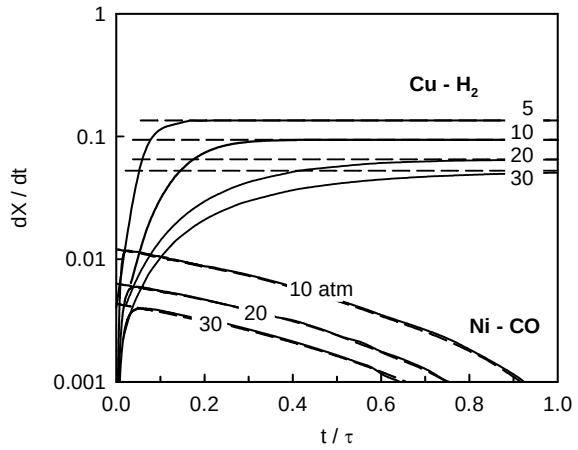

Figure 8. Effect of the gas dispersion in the system on the CGSM predictions for different oxygen carriers reactivities and total pressures. Continuous lines= model predictions considering gas dispersion; discontinuous lines= model predictions neglecting gas dispersion.

About design of pressurized CLC. There are in the literature several works related with design of CLC plants. Lyngfelt et al.[34] presented the first design of an atmospheric CLC plant including a high-velocity riser for the air reactor and a low-velocity fluidized bed for the fuel reactor. A conceptual design of a 10-kW thermal power CLC working at atmospheric pressure was done by Kronberger et al.[3] Wolf et al.[17] have recently analyzed the feasibility of CLC in two interconnected pressurized fluidized bed reactors for a capacity of 800 MW input of natural gas. They mentioned the reaction kinetics as one of the most important technical constrains of the oxygen carriers still lacking from the point of view of the system's performance as a consequence of the little data available in the literature.

The results obtained in this work can be useful for the design of pressurized CLC systems considering that the reactivity of the carrier material must allow sufficient reduction and oxidation rates to fulfill the mass and energy balances. These balances are not affected by the pressure, and are only dependent on the type and content of metal oxide existing in the oxygen carrier.

Taking as reference the same thermal power and using the same gas velocity, the diameter of the reactors in a pressurized CLC plant is smaller than in an atmospheric CLC plant. Oppositely to the expected, we have found that an increase in the operating pressure produced a small decrease in the reaction rates of the oxygen carriers. The solids would need higher residence times to fulfill the mass

balance and taller beds would be necessary in a pressurized CLC plant. The solids inventory in the system should be also higher although the exact values will depend on the oxygen carrier used. To better know these values it is not satisfactory to use kinetic parameters obtained at atmospheric pressure. Although an initial approach has been made in this work to consider the effect of the total pressure on the kinetic parameters, it is recommendable to determine them at the operating pressure of the CLC plant.

Conclusions

This work analyses the main features related with the CLC process to use the syngas obtained in an integrated gasification combined cycle (IGCC) power plant. The kinetics of reduction with H_2 and CO, and oxidation with O_2 of three high reactivity oxygen carriers based on Cu, Fe and Ni have been determined by thermogravimetric analysis both at atmospheric pressure and at higher pressures. The kinetic parameters obtained at atmospheric pressure showed a small effect of temperature for the three oxygen carriers, with values of activation energy ranging from 7 to 25 kJ/mol, and reaction orders from 0.25 to 1. No effect of the gas products (CO_2 or H_2O) was detected on the reduction reaction rates.

The pressurized experiments showed that an increase in total pressure has a negative effect on the reaction rate of all oxygen carriers and reactions. The use of the kinetic parameters obtained at atmospheric pressure in the CGSM was unable to predict the experimental results obtained at pressure. In this sense, a sharp decrease in the value of the preexponential factor was observed in the majority of the cases when the pressure changed from 1 to 5 atm, with a smoother decrease for increasing pressures. To obtain those results, it has been considered the gas dispersion existing in the experimental system, which was very important at high pressures and especially for highly reactive materials.

Although it has not been corroborated in this work, it is very probable that the internal structure of the oxygen carriers changes with operating pressure, decreasing the reaction rate of the materials. Therefore, the kinetic parameters necessary to design pressurized CLC systems must be determined at the operating pressure of the industrial plant. Considering the decrease in the reaction rate with

increasing pressure experimentally observed in all the oxygen carriers, higher solids inventories than the initially expected will be necessary for the CLC pressurized operation.

Acknowledgement. This work was carried out with financial support from the European Coal and Steel Community Project (7220-PR125), and the Spanish Ministry of Education and Science (Project PPQ-2001-2111). The authors thank Dr. Anders Lyngfelt and Dr. Tobias Mattisson for the preparation of the freeze-granulated particles.

REFERENCES

(1) Takematsu, T.; Maude, Ch. Coal Gasification for IGCC power Generation. IEA Coal Research: London, 1991.

(2) Riemer, P. *Energy Convers. Manag.* **1996**, 37, 665-670.

(3) Kronberger, B.; Lyngfelt, A.; Löffler, G.; Hofbauer, H. *Ind. Eng. Chem. Res.* **2005**, 44, 546-556.

(4) Copeland, R. J.; Alptekin, G.; Cessario, M.; Gerhanovich, Y. *Proceedings of the First National Conference on Carbon Sequestration,* Washignton, DC, 2001; LA-UR-00-1850.

(5) Jin, H.; Ishida, M. *Fuel* **2004**, 83, 2411-2417.

(6) Jin, H.; Ishida, M. *Proceedings of TAIES´97 International Conference*, Beijing, 1997, pp 548-553.

(7) Wolf, J.; Anheden, M.; Yan, J. *International Pittsburg Coal Conference*, Newcastle, New South Wales, Australia, 2001.

(8) Davidson. J.; Bressan, L.; Domenichini, R. *Proceedings of the 7th International Conference on Grrenhouse Gas Control Technologies* - GHGT-7, Vancouver, 2004.

(9) Lyngfelt, A.; Kronberger, B.; Adánez, J.; Morin, J.-X.; Hurst, P. *Proceedings of the 7th International Conference on Grrenhouse Gas Control Technologies* - GHGT-7, Vancouver, 2004.

(10) Morin, J-X; Beal, C. Chemical-Looping Combustion of Refinery Fuel Gas with CO_2 Capture. In *Carbon Dioxide Capture for Storage in Deep Geologic Formations - Results form the CO_2 Capture Project*. Eds. Thomas, D., Benson, S. Volume 1, Chapter 37. Elsevier Science, London, **2005**.

(11) Mattisson, T.; Järdnäs, A.; Lyngfelt, A. *Energy Fuels* **2003**, 17, 643-651.

(12) Kronberger, B.; Johansson, E.; Löffler, G.; Mattisson, T.; Lyngfelt, A.; Hofbauer, H. *Chem. Eng. Technol.* **2004**, 27, 1318-1326.

(13) Adánez, J.; de Diego, L. F.; García-Labiano, F.; Gayán, P.; Abad, A. *Energy Fuels* **2004**, 18, 371-377.

(14) Adánez, J.; García-Labiano, F.; de Diego, L. F.; Gayán, P.; Abad, A.; Celaya, J. Development of oxygen carriers for chemical-looping combustion. In *Carbon Dioxide Capture for Storage in Deep Geologic Formations - Results form the CO_2 Capture Project*. Eds. Thomas, D., Benson, S. Volume 1, Chapter 34. Elsevier Science, London, **2005**.

(15) Jin, H.; Ishida, M. *Ind. Eng. Chem. Res.* **2002**, 41, 4004-4007.

(16) Ryu, H.-J.; Bae, D.-H.; Lee, S.-Y.; Jin, G.-T. *Theor. Appl. Chem. Eng.* **2002**, 8, 3798-3792.

(17) Wolf, J.; Anheden, M.; Yan, J. *Fuel* **2005**, 84, 993-1006.

(18) Cho, P.; Mattisson, T.; Lyngfelt, A. *Ind. Eng. Chem. Res.* **2005**, 44, 668-676.

(19) García-Labiano, F.; de Diego, L. F.; Adánez, J.; Abad, A.; Gayán, P. *Ind. Eng. Chem. Res.* **2004**, 43, 8168-8177.

(20) Levenspiel, O. *Chemical Reaction Engineering*; John Wiley and Sons: New York, 1981.

(21) Danckwerts, P. V. *Chem. Eng. Sci*. **1958**, 2, 1-13.

(22) Kronberger, B.; Löffler, G.; Hofbauer, H. *Clean Air* **2005**, 6, 1-14.

(23) Georgakis, C.; Chang, C. W.; Szekely, J. *Chem. Eng. Sci.* **1979**, 34, 1072-1075.

(24) Mattisson, T.; Johansson, M.; Lyngfelt, A. *Energy Fuels* **2004**, 18, 628-637.

(25) Adánez, J.; Capture of CO_2 in Coal Combustion. ECSC Final Report. (Project No. 7220-PR125) **2005**.

(26) Matsukata, M.; Ando, H.; Ueyama, K. *Proceedings of the 15th International Conference on Fluidized Bed Combustion*, Savannah, **1999**.

(27) Agnihotri, R.; Chauk, S. S.; Misro, S. K.; Fan, L.-S. *Ind. Eng. Chem. Res.* **1999**, 38, 3802-3811.

(28) Qiu, K.; Lindqvist, O. *Chem. Eng. Sci.***2000**, 55, 3091-3100.

(29) Qiu, K.; Anthony, E. J.; Jia, L. *Fuel* **2001**, 80(4), 549-558.

(30) García-Labiano, F.; Adánez, J.; Abad, A.; de Diego, L. F.; Gayán, P. *Energy Fuels* **2004**, 18, 761-769.

(31) Chauk, S. S.; Agnihotri, R.; Jadhav, R. A.; Misro, S. K.; Fan, L-S. *AIChE J.* **2000**, 46, 1157-1167.

(32) García-Labiano, F.; de Diego, L. F.; Adánez, J.; Abad, A.; Gayán, P. *Chem. Eng. Sci.* **2005**, 60, 851-862.

(33) Adánez, J.; Abad, A.; de Diego, L. F.; García-Labiano, F.; Gayán, P. *Ind. Eng. Chem. Res.* **2004**, 43, 4132-4139.

(34) Lyngfelt, A.; Leckner, B.; Mattisson, T. *Chem. Eng. Sci.* **2001**, 56, 3101-3113.

Nomenclature

a, c = stoichiometric factor, mol of solid produced (mol of gas)$^{-1}$

b = stoichiometric factor, mol of solid reacting (mol of gas)$^{-1}$

d = parameter in eq. (9)

C = gas concentration, mol m^{-3}

C_i = gas concentration at the inlet, mol m^{-3}

C_{eq} = gas concentration at equilibrium conditions, mol m^{-3}

E = activation energy, J mol^{-1}

k = chemical reaction rate constant, $mol^{1-n}\ m^{3n-2}\ s^{-1}$

k_0 = preexponential factor of the chemical reaction rate constant obtained at atmospheric pressure, $mol^{1-n}\ m^{3n-2}\ s^{-1}$

$k_{0,p}$ = preexponential factor of the chemical reaction rate constant for pressurized conditions, $mol^{1-n}\ m^{3n-2}\ s^{-1}$

L = layer thickness of the reacting solid for the plate-like geometry, m

m = mass of sample, g

m_{ox} = mass of the fully oxidized oxygen carrier, g

n = reaction order

P = total pressure, atm

Pp = partial pressure, atm

R = ideal gas constant, $J\ mol^{-1}\ K^{-1}$

R_0 = oxygen transport capacity of the oxygen carrier

r = grain radius, m

t = time, s

T = temperature, K

X = solid conversion

Greek letters

ρ_m = molar density of the reacting material, $mol\ m^{-3}$

τ = time for complete solid conversion, s